into the evolution of the gas with cosmic time. However, this can only be achieved by extending the coverage to lower frequencies. Automated processing of the data from the intial calibration, RFI flagging to imaging will become more relevant with the increase of the sample size and data volume.

As mentioned above, upcoming blind surveys such as SHARP with APERTIF in the northern hemisphere are expected to increase the number of H I absorption detections providing the targets for H I follow-up observations. Making use of the wide-field capabilities provides the means to cover multiple sources with a single observation. Since the sensitivity of H I VLBI observations primarily depends on the number of stations and observing time, it can be improved significantly by joint observations with the VLBA, VLA, LBA and Arecibo. This is particularly useful for detailed single source studies. In the SKA era, joint observation with SKA-MID can provide important *uv*-coverage for lower declination sources as well as a significant boost in sensitivity.

Understanding the physics of gaseous matter also requires knowledge of other gas tracers. In terms of the cold molecular gas, they can be obtained almost at a comparable resolution by ALMA and NOEMA. The powerful combination of H I and molecular gas has already been demonstrated in several cases (e.g. Morganti et al. 1998; Tadhunter et al. 2014; Maccagni et al. 2016; Oosterloo et al. 2017). For example, Tremblay et al. (2016) used information from both tracers to show the occurence of chaotic accretion in the Bright Galaxy Cluster Abell 2597 (see Fig. 2.11). The outflowing H I gas in Mrk 231 is likely driven by radiation pressure rather than the jet. Outflows of molecular and atomic gas seem to be more massive than those of ionised gas (e.g. Morganti 2017 and references therein). However, the sample size for outflows of cold gas is still limited and future observations will have to show whether this holds. Molecular absorption has been detected with VLBI, too, for example recently with the KVN in NGC 1052 (Sawada-Satoh et al. 2016).

The radio telescopes comprising the EVN primarily cover the northern hemisphere. As such H I VLBI greatly benefits from the wealth of optical information available from SDSS (Abolfathi et al. 2017) and in the future WEAVE which will perform follow-up of the APERTIF and LOFAR surveys. The gas close to the AGN may also be probed with soft X-ray observations and joint X-ray and H I absorption studies will become more important with the upcoming survey conducted by *eROSITA* (e.g. Moss et al. 2017).

As mentioned earlier, there is a close connection to numerical simulations at high-spatial resolution. H I continues to remain almost the only observational technique to provide constraints at comparable resolution. With the advances in computing power and theoretical models, we are confident that these simulations will be able to better incorporate the cold gas.

References

Abolfathi, B. et al., 2018, *ApJS*, **235**, 42
Antonucci, R., 1993, *Ann. Rev. Astr. Astrophys.*, **31**, 473
Araya, E. D. et al. 2010, *AJ*, **139**, 17
Argo, M. K. et al., 2010, *MNRAS*, **402**, 2703
Argo, M. K., 2018, *IAU Symp.*, **336**, 121
Baldi, R. et al., 2018, *MNRAS*, **476**, 3478
Beswick, R. J. et al., 2015, *POS["AASKA14"]70*
Beswick, R. J. et al., 2015, *POS["Many Facets of extragalactic radio surveys"]13*
Biggs, A. D. et al., 2016, *MNRAS*, **462**, 2819
Bondi, M. et al., 2012, *A&A*, **539**, 134
Burtscher, L. et al., 2013, *A&A*, **558**, A149

Castangia, P. et al., 2019, *A&A*, **629**, A25
Chapman, S. C. et al., 2003, *ApJ*, **585**, 57
Chi, S., Barthel, P. D., & Garrett, M. A., 2013, *A&A*, **550**, A68
Curran, S. J., 2017, *A&A*, **606**, A56
Curran, S. J., & Duchesne, S. W., 2018, *MNRAS*, **476**, 3580
Di Matteo, S. et al., 2005, *Nature*, **433**, 604
Espada, D. et al., 2010, *ApJ*, **720**, 666
Falcke, H. Körding, E., & Markof, S., 2004, *A&A*, **414**, 895
Fenech, D. M. et al., 2010, *MNRAS*, **408**, 607
Field, G. B., 1959, *ApJ*, **129**, 536
Gallimore, J. F. et al., 2001, *ApJ*, **556**, 694
Galvin, T. J. et al., 2016, *MNRAS*, **461**, 625
Gao, F. et al., 2017, *ApJ*, **835**, 52
Gray, M. D., 2007, *MNRAS*, **375**, 477
Greenhill, L. J. et al., 2003, *ApJ*, **590**, 162
Gruppioni, C. et al., 2017, *PASA*, **34**, 55
Gupta, N. et al., 2018, *MNRAS*, **476**, 2432
Herzog, A. et al., 2015, *A&A*, **578**, A67
Hoenig, S. F., & Kishimoto, M. 2017, *ApJ*, **838**, L20
Holt, J. et al., et al., 2006, *MNRAS*, **370**, 1633
Hopkins, A. M., & Beacom, J. F., 2006, *ApJ*, **651**, 142
Kamali, F. et al., 2019, *A&A*, **624**, A42
Katsianis, A. et al., 2017, *MNRAS*, **464**, 4977
Kistler, M., D. et al., 2009, *ApJ*, **705**, 104
Kloeckner, H. R., Baan, W. A., & Garrett, M. A. 2003, *Nature*, **421**, 821
Kondratko, P. T., Greenhill, L. J., & Moran, J. M. 2005, *ApJ*, **618**, 618
Kuo, C. Y. et al., 2011, *ApJ*, **727**, 20
Leahy, D. & Tian, W., 2010, *ASP Conf. Ser.*, **438**, 365
Lo, K. Y. 2005, *Ann. Rev. Astr. Astrophys.*, **43**, 625
Maccagni, F. M. et al., 2017, *A&A*, **604**, A43
Maccagni, F. M. et al., 2016, *A&A*, **588**, A46
Madau, P. & Dickinson, M., 2014, *ARA&A*, **52**, 415
Mezcue, M. et al., 2015, *MNRAS*, **448**, 1893
Middelberg E. et al., 2008, *A&A*, **491**, 435
Morganti, R., 2017, *Frontiers in Astronomy and Space Sciences*, **4**, 42
Morganti, R. et al., 2013, *Science*, **341**, 1082
Morganti, R. & Oosterloo, T., 2018, *A&AR*, **26**, 4 [arXiv:1807.01475]
Morganti, R. et al., 2018, *Proceedings of IAU-S342, Perseus in Sicily: from black holes to cluster outskirts*, eds. K. Asada, E. de Gouveia dal Pino, H. Nagai, R. Nemmen, M. Giroletti [arXiv:1807.07245]
Morganti, R., Oosterloo, T., & Tsvetanov, Z., 1998, *AJ*, **115**, 915
Morganti, R. et al., 2009, *A&A*, **505**, 559
Morganti, R., Sadler, E. M., & Curran, S. 2015, *PoS["AASKA14"]134*
Morganti, R. et al., 2016, *A&A*, **593**, A30
Morrison, G. et al., 2008, *ASPC*, **381**, 376
Moss, V. A. et al., 2017, *MNRAS*, **471**, 2952
Mukherjee, D. et al., 2016, *MNRAS*, **461**, 967

Mukherjee, D. et al., 2017, *MNRAS*, **471**, 2790
Mukherjee, D. et al., 2018, *MNRAS*, **476**, 80
Murphy, E. J. et al., 2017 *ApJ*, **839**, 35
Muxlow, T. W. B. et al., 2006, *PoS["8thEVN"]31*
Muxlow, T. W. B. et al., 2005 *MNRAS*, **358**, 1159
Muxlow, T. W. B. et al., 2010, *MNRAS*, **404**, 109
Nagar, N. M., Falcke, H., & Wilson A. S, 2005, *A&A*, **435**, 521
Oosterloo, T. et al., 2017, *A&A*, **608**, A38
Padovani, P. et al., 2015, *MNRAS*, **452**, 1263
Park, S. et al., 2017, *MNRAS*, **465**, 3943
Peck, A. B. et al., 2003, *ApJ*, **590**, 149
Pérez-Torres, M. A. et al., 2009, *A&A*, **507**, L17
Pérez-Torres, M. A. et al., 2010, *A&A*, **519**, L5
Pihlstroeom, Y. M. et al., 2001, , *A&A* **377**, 413
Pope, A. et al., 2006, *MNRAS*, **370**, 1185
Radcliffe, J. F. et al., 2018, *A&A*, **619**, A48
Ramos Almeida, C., & Ricci, C., 2017, *Nature Astronomy*, **1**, 679
Richards, E. A. et al., 1998, *AJ*, **116**, 1039
Sawada-Satoh, S. et al., 2016, *ApJ*, **830**, L3
Schilizzi, R. T. et al., 2001, *A&A*, **368**, 398
Schulz, R. et al., 2018, *A&A*, **617**, A38
Smolčić, V. et al., 2017, *A&A*, **602**, A6
Srianand, R. et al., 2015, *MNRAS*, **451**, 917
Staveley-Smith, L. & Oosterloo, T., 2015, *PoS["AASKA14"]167*
Struve, C. & Conway, J. E., 2010, *A&A*, **513**, A10
Struve, C. & Conway, J. E. 2012, *A&A*, **546**, A22
Struve, C. et al., 2010, *A&A*, **515**, A67
Tarchi, A. 2012, *IAU Symp.*, eds. R. S. Booth, W. H. T. Vlemmings, & E. M. Urry, C. M., & Padovani, P. 1995, *PASP*, **107**, 803
Tadhunter, C. et al., 2014, *Nature*, **511**, 440
Taylor, G. B. et al., 1999, *ApJ*, **512**, L27
Tremblay, G. R. et al., 2016, *Nature*, **534**, 218
Varenius, E. et al., 2019, *A&A*, 623, A173
Westcott et al., 2018, *MNRAS*, **475**, 5116
Wills, K. A. et al., 2000, *MNRAS*, **316**, 33
Yang et al., 2017, *MNRAS*, **464**, 70
Zhao, W. et al., 2018, *ApJ*, **854**, 124

3. Innermost regions of AGN

Active galactic nuclei are key targets of very long baseline interferometry. The mas-scale angular resolution provided by VLBI allows not only to unveil the AGN physcis and energy transport in the vicinity of supermassive black holes (SMBH) responsible for their activity, but also to address the question of their evolution with cosmic time and co-evolution with the host galaxy. These two topics are addressed in the following sections.

3.1 Active Galactic Nuclei

The current astrophysical paradigm firmly sets galactic activity and active galactic nuclei among the most important factors affecting galaxy evolution and large scale structure in the Universe on cosmological scales. Galactic activity is closely related to the presence of supermassive black holes which are now believed to be residing in the centres of all spiral and elliptical galaxies. Energy generated through matter accretion onto SMBH is released and transported outward in form of broadband continuum radiation and kinetic energy vested into nuclear outflows. In a subset of *radio-loud* AGN, a fraction of the outflowing material is organised in highly collimated, relativistic jets. The jets are responsible for a large fraction of non-thermal continuum emission (particularly during powerful flares), which makes understanding their physics an important aspect of studies of AGN characterised by profound flaring activity arising from extremely compact regions. High-resolution observations of extragalactic jets with very long baseline interferometry (VLBI) offer arguably the best tool to understand their physics down to the smallest spatial scales and to use them as effective probes of the extreme vicinity of central black holes in AGN (see Boccardi et al. 2017 for review).

3.1.1 Central regions of radio-loud AGN

The central region of radio-loud AGN manifest a complex interplay between several major constituent parts, including the black hole and its magnetosphere, the accretion disk and the hot, non-thermal

Chapter image credit: NASA / JPL-Caltech.
From: `https://photojournal.jpl.nasa.gov/catalog/PIA16695` .

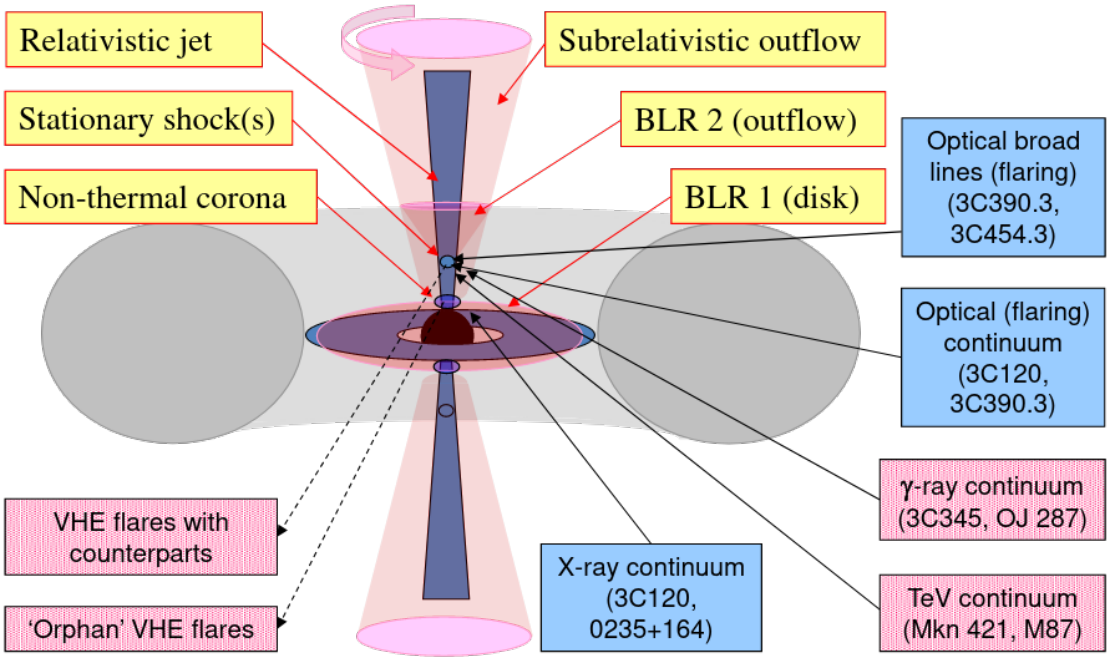

Figure 3.1: Schematic view of the central region of a radio-loud AGN. The overall manifestation of nuclear activity results from a complex interplay between the black hole, accretion disk, non-thermal corona, broad-line emitting region, and relativistic jets. In radio-loud AGN, jets either produce or influence the production of a large fraction of non-thermal continuum, as indicated by the examples shown in the figure and resulting from VLBI-based investigations of individual objects (for details, see Acciari et al. 2010, Arshakian et al. 2010, León-Tavares et al. 2010, 2013, Agudo et al. 2011, Schinzel et al. 2012, Jorstad et al. 2013, Hada et al. 2014).

corona, and the broad-line emitting clouds (Fig. 3.1). Each of the major AGN constituents contributes to a specific domain in the broad-band spectral energy distribution (Ghisellini & Tavecchio 2009), and most of them can be probed through their interaction with relativistic jets produced in radio-loud galaxies.

Relativistic jets form in the vicinity of central black holes, with ample evidence connecting their formation and propagation to physical conditions in the accretion disc and broad-line region (cf., Arshakian et al. 2010, León-Tavares et al. 2010, Hada et al. 2014). Imaging and polarimetry of radio emission on milliarcsecond scales provided by very long baseline interferometry (VLBI) offers a range of possibilities for studying ultra-compact regions in relativistic jets (*e.g.*, Gómez et al. 2016) and relating them to main manifestations of activity in AGN.

Simultaneous monitoring of the optical and high energy variability and the evolution of parsec-scale radio structures yields a detailed picture of the relation between acceleration and propagation of relativistic flows and non-thermal continuum generation in active galaxies (cf., Acciari et al. 2010, Arshakian et al. 2010, León-Tavares et al., 2010, 2013, Jorstad et al. 2013, Hada et al. 2014). Opacity effects provide a measure of magnetic field strength on scales down to ~ 1000 gravitational radii, $R_{\rm g}$, and trace the distribution of broad-line emitting material (Lobanov 1998, Fromm et al. 2013).

Correlations observed between parsec-scale radio emission and optical and gamma-ray continuum indicate that a significant fraction of non-thermal continuum may be produced (particularly during flares) in extended regions of relativistic jet at distances up to 10 parsecs from the central engine (Agudo et al. 2011, Schinzel et al. 2012). Combined with studies of jet component ejections and X-ray variability, these correlations also suggest that time delays, nuclear opacity, and jet acceleration may have a pronounced effect on the observed broad-band variability and instantaneous spectral energy distribution (León-Tavares et al. 2010). A number of recent studies, combining VLBI polarisation and opacity measurements with multi-band information provide an ever growing support for magnetic fields as one of the most important factors governing the generation and outward transport of the energy in AGN (cf., Zamaninasab et al. 2014, Baczko et al. 2016, Mertens et al. 2016, Walker et al. 2018)

These examples demonstrate that VLBI observations of relativistic jets remain a unique tool of choice for localising, classifying, and investigating the broadband continuum and broad spectral line emission produced in AGN. This unique position of VLBI is solidly based on its unmatched capability observation to provide two-dimensional and time-dependent kinematic, spectral, and polarisation information about regions down to the immediate vicinity of the central black holes in AGN. Future directions of the EVN research should fully exploit and enhance this capability.

3.1.2 Jet physics from VLBI observations

Jets in active galaxies are formed in the immediate vicinity of the central black hole, at distances of 10–$10^2\,R_\mathrm{g}$ (Camenzind 2005, Meier et al. 2009). The jets carry away a fraction of the angular momentum and energy stored in the accretion flow (Blandford & Payne 1982), the non-thermal corona (in low luminosity AGN; Merloni & Fabian 2002), or the rotating magnetosphere of the central black hole (Blandford & Znajek 1977).

Table 3.1: Spatial, temporal, and emission scales in jets

Region	**Characteristic scales**				ν_m
	Natural [R_s]	Linear [pc]	Angular	Temporal	[GHz]
Launching	10–10^2	10^{-4}–10^{-3}	0.02–0.2 μas	1.5–15 h	>100
Collimation	10^2–10^3	10^{-3}–10^{-2}	0.2–2.0 μas	0.6–6 d	50–100
Acceleration	10^3–10^6	10^{-2}–10^1	0.02–2.0 mas	0.25–17 y	10–50
Propagation	10^6–10^{10}	10^1–10^5	0.005–20″	17–17000 y	0.1–10
Dissipation	10^{10}–10^{11}	10^5–10^6	0.33–3.3′	0.17–1.7 My	<0.1

Notes: Scales are calculated for a $10^8 M_\odot$ AGN at a distance of 1 Gpc (these also correspond to a $10\,M_\odot$ XRB at a distance of 100 pc) The temporal scales pertain to the light crossing times of the respective length scales. The peak frequency ν_m gives an approximate range for the synchrotron turnover frequency.

In all of these mechanisms, electromagnetic processes and magnetic fieldss in particular play a pivotal role in launching, collimating, and accelerating the jets on scales of up to $10^6\,R_\mathrm{g}$ (cf., Komissarov et al. 2007, Lyubarsky 2009, Fendt 2011, Marscher 2014). This calls for particular attention to multi-frequency VLBI observations recovering broadband spectrum, polarisation, opacity, and internal structure of the flow on these scales.

A sketch of an extragalactic jet shown in Fig. 3.2 in comparison to the typical resolution of VLBI observations, and basic properties of different jet regions summarised in Table 3.1 indicate

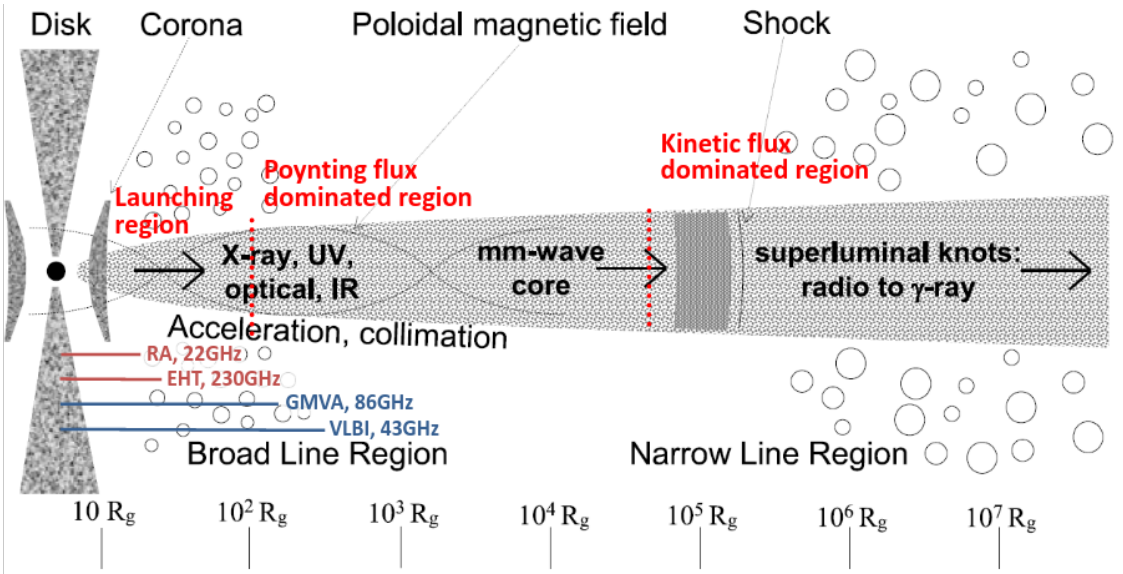

Figure 3.2: Sketch of a relativistic jet in AGN in relation to other constituents of the central region and a typical resolution of different VLBI instruments when targeting a nearby object such as M 87. The global VLBI at 43 GHz is sufficient to probe well into the jet collimation and acceleration region, and space VLBI observations with *RadioAstron* at 22 GHz could resolve even the jet launching region. These observations however may be hindered by the opacity in the jet and in the ambient medium. Observing at higher frequencies with the GMVA and EHT should alleviate this problem.

that effective studies of jet launching and formation should be done at frequencies above 22 GHz, while the jet propagation is best assessed at lower frequencies.

RadioAstron observations of 3C 84 at 22 GHz (Fig. 3.3) and multi-frequency measurements of the jet collimation and velocity field (Fig. 3.4 in M 87 exemplify the effectiveness of high-fidelity VLBI observations for studying these regions of the flow. These observations suggest that the jet may indeed tap their energy from both the accretion disk and the magnetosphere of the black hole (cf., Hardee et al. 2007). Further support for this idea comes from multi-frequency polarisation studies (cf., Gabuzda et al. 2014, Molina et al. 2014) indicating the likely presence of helical magnetic fields in the jets on these linear scales.

To be effective in future studies of this kind, VLBI observations should put the main emphasis on achieving high-fidelity polarisation measurements at multiple bands, warranting a true two-dimensional recovery of the spectral and magnetic field information. With this approach, it would become possible to understand the role and relative contribution of the accretion disk and black hole magnetosphere to the jet formation, and to look for the elusive non-thermal corona in low-luminosity AGN, and to distinguish between different scenarios of jet propagation and energy release.

3.1.3 Immediate vicinity of event horizon scales

Direct imaging of the event horizon scales is currently one of the prime goals of VLBI studies of AGN, with the focus of attention firmly laid on the Event Horizon Telescope (Doeleman et al. 2012) observing the central black holes in Sgr A* and M 87 at 230 GHz. While holding the best promise for revealing a compelling evidence for the existence of the event horizon, the EHT observations

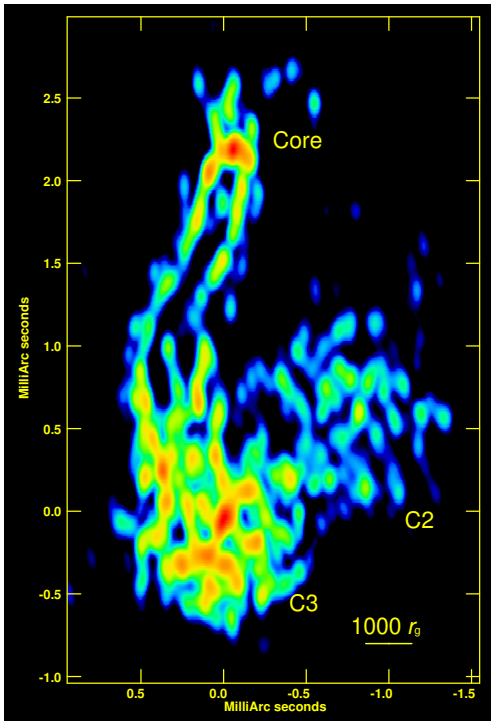

Figure 3.3: Inner jet in 3C 84, observed at 22 GHz with *RadioAstron* (Giovannini et al. 2018). The jet is transversally resolved and shows an extremely rapid collimation into an essentially cylindrical profile with a transverse radius of $\sim 250\,R_{\rm g}$. This suggest either an extremely rapid lateral expansion of a magnetospheric (Blandford-Znajek) jet or the launching of the jet from the accretion disk (via Blandford-Payne mechanism).

alone may not necessarily be able to distinguish a true black hole from one of its "mimickers" such as, for instance, the gravastar (cf., Chirenti & Rezzolla 2017).

High-sensitivity and high-fidelity GMVA observations at 86 GHz already now can help discriminating between different models for the jet formation (Fig. 3.5). These observation also provide a much needed input for physical modelling of the data from the EHT observations at 230 GHz including the information about the jet rotation, and velocity distribution (cf., Mertens et al. 2016, Walker et al. 2018). Further improvements of the dynamic range of GMVA observations will result in increasing the effective image resolution of VLBI images at 86 GHz, providing a much more detailed support for modelling jets and recovering physical information from EHT images.

An even more important contribution to studies of the event horizon scales in AGN would be provided by dedicated measurements of magnetic field strength and structure made on scales below $\sim 1000\,R_{\rm g}$, where the maximum magnetic field of $\sim 10^4$ G expected for the black hole scenario can be effectively contrasted with much stronger dipole fields expected for most of the black hole alternatives (Lobanov 2017). Effective measurements of magnetic fields on scales of $< 1000\,R_{\rm g}$

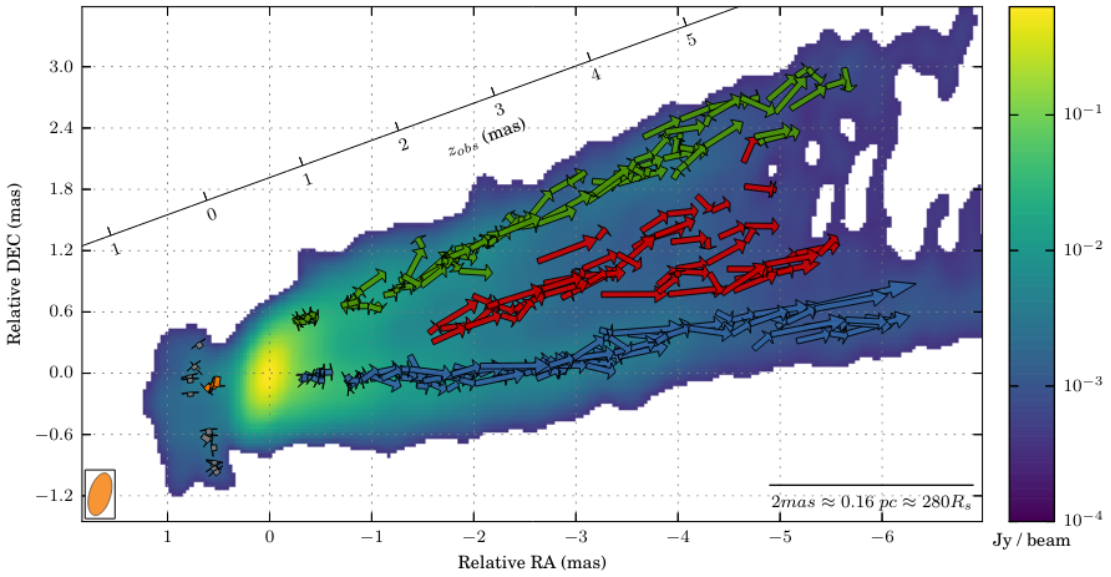

Figure 3.4: Two-dimensional velocity distribution in the jet M 87 obtained from wavelet-based decomposition of a sequence of VLBI images at 43 GHz. The velocity field reveals the presence of two distinct velocity components and, combined with the collimation profile of the flow strongly suggests that the jet launching occurs both at the accretion disk and near the black hole magnetosphere, with the latter flow reproducing the faster spine of the flow. Credit: Mertens et al. (2016), reproduced with permission ©ESO.

can be enabled by making detailed VLBI observations of polarisation (cf., Gómez et al. 2016), Faraday rotation (cf., Gabuzda et al. 2014, Molina et al. 2014) and opacity (cf., Kovalev et al. 2008, Pushkarev et al. 2012, Fromm et al. 2013, Plavin et al. 2019).

3.1.4 Main research directions for the coming decade

Enabling robust, frequency agile, polarimetric VLBI operations in the 1.6–86 GHz range of frequencies will provide an excellent foundation for addressing a number of outstanding fundamental questions about physics of relativistic jets and cosmic black holes, as well as the role they are playing in shaping up the galactic activity. Starting from these premises, one can identify three major areas of engagement for VLBI studies of relativistic jets to be made in the coming decade:

1. Multi-band observations at frequencies below 22 GHz would give ultimate answers about the physical mechanisms of jet collimation and acceleration.
2. Systematic studies of internal structure, velocity fields and their evolution would provide the clues necessary to assess the role and relative prominence of the Blandford-Payne and Blandford-Znajek mechanisms of energy extraction from accreting black holes. Extending such VLBI studies to low luminosity jets should also give better understanding of the physical nature of the non-thermal corona believed to be playing a crucial role in shaping the activity in radio-quiet AGN.
3. Dedicated imaging programmes at 86 GHz and systematic measurements of magnetic field strength and structure on linear scales below 1000 R_g would provide crucial information about the jet launching and the physical nature of cosmic black holes.

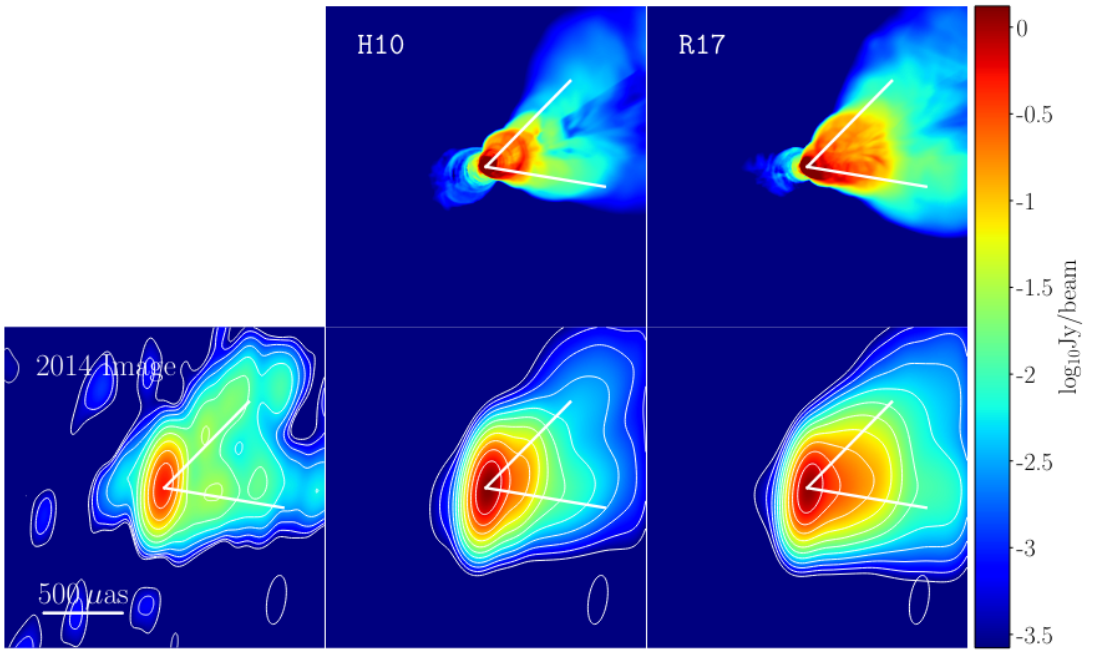

Figure 3.5: GMVA image of M 87 (lower left panel; Kim et al. 2018, reproduced with permission ©ESO) contrasted with results of numerical simulations of a jet produced from a two-temperature magnetically arrested disk (Adapted Fig. 12 from Chael et al. 2019). The full resolution frames of two specific models (top frames) are shown in the bottom row after being convolved with the same restoring beam as in the real VLBI image. Limited conclusions about the preferred scenario can already be made from the analysis of the internal structure of the jet, slightly favoring the H10 model (see Chael et al. 2019 for details of the modelling). Improving the dynamic range and fidelity of GMVA imaging would increase the effective resolution of 86 GHz VLBI images and provide much stricter constraints on the physical models.

3.1.5 VLBI at microarcsecond resolution

Successful engagement with the fundamental issues identified above relies on steady improvement of technical and imaging capabilities of VLBI measurements. Effective studies of the event horizon scales require VLBI imaging at a $\sim 10\,\mu$as resolution and sensitive to smooth emission on angular scales up to ~ 5 mas. Such requirements impose stringent constraints not only on thermal noise sensitivity but also on the phase stability and *uv*-coverage of VLBI observations.

At frequencies below 15 GHz, the planned development of the BRAND receiver (tuccari et al. 2017) should provide excellent frequency coverage and agility while maintaining the detection sensitivity. At higher frequencies steady increase of the observing bandwidth will bring further reduction of the thermal noise and improve the detection threshold. However, as the image dynamic range equally depends on the phase noise, other factors contributing to it should also be dealt with.

Reducing the amplitude noise, $\sigma_{\rm amp}$, increases the effective resolution $\theta_{\rm res} \propto FWHM_{\rm beam}\sqrt{\sigma_{\rm amp}}$. Conversely, reduction of phase noise, $\sigma_{\rm phas}$ improves positional accuracy, $\Delta_{\rm pos} \propto FWHM_{\rm beam}\sigma_{\rm phas}$. A potentially very powerful way to achieve both these improvements is offered by the multi-frequency (22/43/86/129 GHz) receiver technology (Han et al. 2013) developed at the Korean VLBI Network

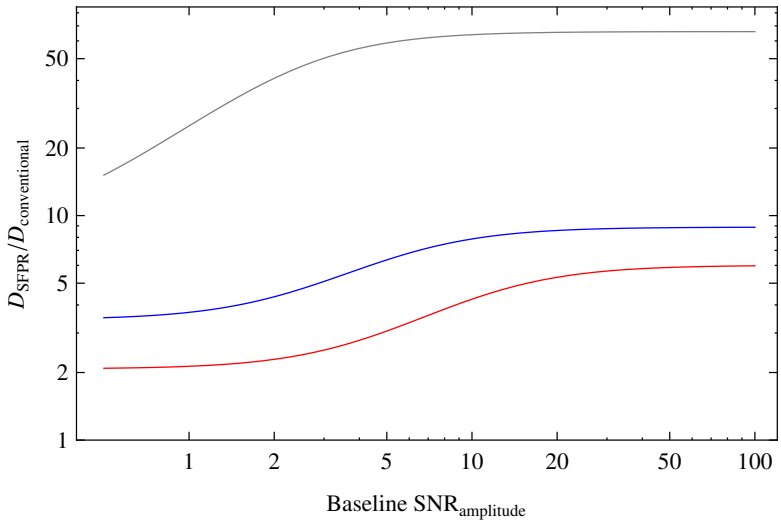

Figure 3.6: Dynamic range of SFPR imaging compared to conventional imaging. The comparison is done as a function of the average SNR of visibility amplitudes in the VLBI data. Quite expectedly, the largest improvement is realised for high amplitude SNR data, and it can reach a factor of 50 for imaging with the EHT.

(KVN). The source frequency phase-referencing technique (SFPR, Rioja et al. 2015) enabled by this receiver has already allowed the KVN to achieve a $\sim 30\,\mu$as astrometric accuracy on a ~ 500 km baseline (cf., Dodson et al. 2017). Further improvements are expected on the imaging dynamic range (Zhao et al. 2018), once it is implemented on a full-fledged imaging VLBI array.

Improvements of image dynamic range expected from implementation of the SFPR for imaging are shown in Fig. 3.6 for VLBI observations at 43, 86, and 230 GHz. The strongest improvement is achieved for imaging with high SNR of the amplitudes and for EHT it can reach a factor of 50, while an order of magnitude improvement is expected for the GMVA observations.

A minimum option of equipping a few EVN antennas with dual (22/43) or triple (22/43/86) frequency modification of the KVN receiver design would readily improve positional measurements, achieving a $\sim 10\,\mu$as astrometric accuracy. Enabling the SFPR option on an imaging array such as the GMVA, the VLBA, or the EAVN(+EVN) would substantially improve fidelity and effective resolution of imaging. The expected effective resolution of 86 GHz VLBI imaging may even exceed that of the present EHT observations, which would revolutionise both the GMVA and the EHT measurements, as discussed in Jung et al. (2015).

3.1.6 Conclusions and recommendations

Dedicated and systematic observations of relativistic jets performed at frequencies between 1.6 and 86 GHz hold an excellent potential to address several outstanding fundamental questions about the jet physics and physical conditions in the immediate vicinity of the supermassive black holes in AGN. These measurements may also hold the best clue about the very nature of the cosmic black holes. The success of these studies relies on the continued technical progress in VLBI observations and imaging. The advances offered by the developments of broadband (BRAND) and multi-band

(KVN) receiver technology would provide revolutionise VLBI imaging in the 1.6–86 GHz regime and they should be considered for a broad implementation at the active VLBI instruments.

3.2 High-redshift AGN and SMBH growth

Quasars are the most prominent AGN, and in fact they are the most powerful non-transient objects in the Universe. Because of their extreme luminosities, they can nowadays be detected from vast cosmological distances. The current record holder is J1342+0928 at redshift $z = 7.54$, corresponding to the cosmological epoch when the Universe was just at 5% of its present age (Bañados et al. 2018b). Radio-loud (or, by adopting the more physically motivated term, jetted; Padovani 2017) quasars constitute the minority ($\leq$10%) of the population. However, from VLBI point of view, they are important observational targets because their structures can be imaged with the finest details, surpassing the resolution offered by any other astronomical technique. The most distant jetted AGN currently known is J1429+5447 at $z = 6.21$ (Willott et al. 2010; Frey et al. 2011). While high-resolution radio interferometric studies of jetted AGN at any redshift in general provide a wealth of unique information on the physical and geometric properties of jets, the accretion onto SMBHs, the jet launching and the emission mechanisms, these objects at very high redshifts ($z > 3-4$) are of particular interest from a couple of points of view. First of all, they should represent the earliest phases of SMBH activity in AGN. Therefore they are crucial for understanding the cosmological evolution of SMBHs and their co-evolution with the host galaxies. On the other hand, high-redshift AGN are promising probes of cosmological models (see e.g. Melia & Yennapureddy 2018, for a recent review). In the subsequent sections we describe high-redshift quasars, as well as peculiar types of AGN (dual/multiple systems; intermediate-mass black holes) that are important targets for the understanding of SMBH growth and evolution.

3.2.1 Blazars as tracers of high-redshift jetted AGN

At low redshifts, the jetted AGN are observed to be $\sim$10% of the total AGN population. Assuming reasonable values for the jet beaming angle ($\sim 3^\circ - 7^\circ$), simple geometrical considerations and an isotropic distribution of jet orientations, we expect that around 1–2 out of 200 jetted sources have their jets aligned close to our line of sight, i.e. can be classified as *blazars*. This source ratio is well proven by comparing high-energy blazar catalogues (such as *Fermi*/LAT catalogues; Atwood et al. 2009, Ackermann et al. 2011) with radio and optical quasar catalogues (such as SDSS+FIRST surveys; York et al. 2000, Shen et al. 2011), that include misaligned blazar counterparts and non-jetted analogous sources. All-sky high-energy catalogues are not able to go beyond $z \sim 3.5$, so to verify this relation, a systematic search of jetted sources was needed. In particular, blazars are extremely efficient tracers for the overall jetted population: the observation of a single blazar under a viewing angle smaller than its jet beaming angle ($\theta_v \leq \theta_b \simeq 1/\Gamma$, where $\Gamma \sim 10-15$ is the bulk Lorentz factor of the emitting region) implies the presence of $2\Gamma^2 \sim 200-450$ analogous jetted sources with their jets directed randomly in the sky. For each blazar with specific mass, accretion rate and jet power, we can infer the existence of hundreds of radio sources with the same mass, accretion rate and jet power, only with their jets directed elsewhere. For a few years, this approach has been applied to high-redshift catalogues, to study the high-redshift jetted AGN population.

From the early 2000s, a large collection of active SMBHs with masses comparable or larger than $10^9\,M_\odot$ has been observed, hosted in bright quasars up to redshift 7. Currently, around 200–300 sources have been identified at $z > 6$, mainly radio-quiet or silent. If the occurrence of jetted sources in the AGN population at such high redshifts is comparable with that of the low redshift population,

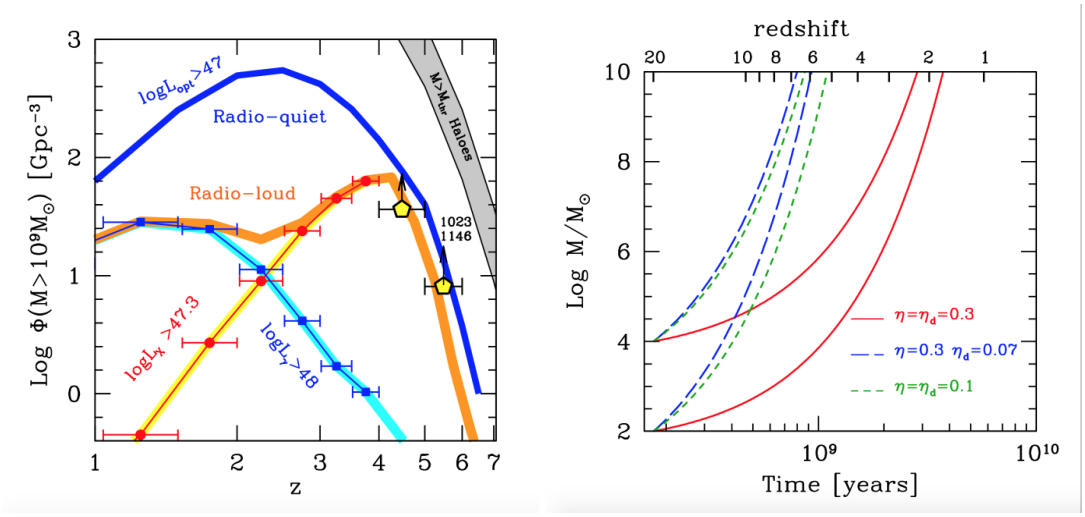

Figure 3.7: *Left panel:* comoving number density of active SMBHs with masses $> 10^9\,M_\odot$ hosted in non-jetted (blue line) and jetted quasars (orange line; Fig. 41 from Sbarrato et al. 2015). Blue points and cyan line are derived from the *Fermi*/LAT all-sky blazar catalogue, while red points and yellow line come from the *Swift*/BAT blazar catalogue. Yellow pentagons are derived from blazars classified through X-ray observations performed on blazar candidates at $z > 4$. *Right panel:* mass of a SMBH accreting at the Eddington limit as a function of time and redshift. Accretion is bound to start at $z = 20$ from a black hole seed of $10^2\,M_\odot$ or $10^4\,M_\odot$ with different efficiencies. Larger η_d values correspond to a smaller amount of mass accreted on the black hole itself. If the fraction of gravitational energy released (η) contributes both to radiation (η_d) and energy launching a jet, the growth time decreases (Fig. 3, Ghisellini et al. (2013).

less than 10% should show a jet, and none of them is expected to point towards our line of sight. At $z > 4$, the number of bright quasars significantly increases up to 1248 objects in the SDSS+FIRST quasar catalogue whose footprint is $\sim 1/4$ of the sky (Shen et al. 2011). For this reason, the search for very high-redshift blazars has been performed starting from this redshift range.

Blazar candidates are selected from SDSS+FIRST survey as extremely radio-loud quasars. Dedicated X-ray observations are then performed, in order to confirm their blazar nature. A hard and strong X-ray spectrum is the unmistakable signature of high-energy emission from a jet aligned to our line of sight. A detailed broad-band spectral energy distribution (SED) fitting helps in constraining SMBH accretion and jet emission features, including viewing angle and bulk Lorentz factor. Currently 8 sources have been classified as blazars in the SDSS+FIRST spectroscopic survey (Sbarrato et al. 2012, 2013, 2015; Ghisellini et al. 2014, 2015) that allow to infer the presence of ~ 2700 jetted quasars with masses $> 10^9\,M_\odot$, accreting at around 10% of the Eddington limit only in the SDSS+FIRST sky area. The results of these classifications allow us to study the comoving number density of active massive black holes at high redshift, and compare the jetted and non-jetted populations. The left panel of Fig. 3.7 shows that the comoving number density of active $> 10^9\,M_\odot$ SMBHs hosted in jetted AGN peak around $z > 4$, much earlier than non-jetted sources of same SMBH mass, that peak at $z \sim 2.5$. This is extremely interesting and challenging from the point of view of early SMBH formation: is it possible to have more jetted than non-jetted AGN in the early Universe?

The large amount of high-redshift very massive quasars already puzzles the AGN community, since such extreme masses are difficult to assemble in the short amount of time available for these sources to evolve (at $z \sim 6$ the age of the Universe is only 900 Myr). Introducing a predominant presence of jets in this puzzle might complicate the already existing issue. The right panel of Fig. 3.7 shows that a non-spinning SMBH accreting at the Eddington limit from a seed of $10^2\,M_\odot$ in standard conditions (i.e. with a radiatively efficient standard accretion disk that releases a fraction $\eta = 0.1$ of its gravitational energy in radiation) is hardly able to build up $10^9\,M_\odot$ before $z \sim 6$ (green short dashed line). In the case of $z \sim 4$ sources, these assumptions hold. Jets, though, are generally associated to highly spinning black holes, and therefore a release of gravitational energy $\eta = 0.1$ typical of non-spinning black holes is not acceptable. The radiative efficiency associated with a maximally spinning black hole is much larger, of the order of $\eta = 0.3$. This means a much smaller amount of mass accreted on the black hole at fixed luminosity (Eddington-limited) in the same amount of time. In other words, maximally spinning black holes are bound to accrete much slower, and blazars such as the ones classified in the last years cannot be assembled before $z \sim 2.5-3$ (red solid lines). This problem can be solved if a fraction of the gravitational energy released during the accretion goes into launching the relativistic jet, instead of being only radiated away. In other words, the release of gravitational energy follows $\eta = 0.3$, but only a fraction of it is radiated from the accretion disk, mimicking the emission from a non-spinning black hole ($\eta_{\rm d} = 0.1$). For an Eddington-limited luminosity, this assumption allows the black hole to accrete faster (long dashed blue line in right panel of Fig. 3.7). This extremely simple toy model gives a new view on the larger comoving number density of massive jetted sources at high redshift: the jet might actually be a way to accrete faster at a fixed accretion luminosity.

The blazars observed up to now in the X-rays have been lately complemented with high-resolution VLBI observations, as summed up in Coppejans et al. (2016). Most sources can be confirmed as blazars with this approach, such as J1026+2542 at $z = 5.266$ (Sbarrato et al. 2012, 2013) that even shows signs of jet component proper motion (Frey et al. 2015). But few of them show different features in radio than at high energies. J1420+1205 ($z = 4.034$) is the most striking example, clearly showing two distinct components in VLBI data (Cao et al. 2017), with clear signatures of being a misaligned source with respect to our line of sight. This inconsistency between high- and low-frequency results might be ascribed to the bending of the jet in a given source, or even to new emitting features for very high redshift sources.

VLBI observations are therefore key in solving these riddles hidden in the early Universe. How many jetted sources are really present? What does the jet emission look like at all scales at very high redshift? High-resolution VLBI observations pushed to lower flux density limits, combined with wider frequency-range X-ray spectroscopy will be instrumental to better understand jet emission and launching mechanisms, hopefully even in connection with SMBH accretion physics.

3.2.2 High-redshift AGN observations with VLBI

Since the early 2000s, following their optical spectroscopic discoveries, the majority of the presently known radio quasars at $z \approx 6$ have been observed with the EVN at 1.6 and/or 5 GHz (J0836+0054 at $z = 5.82$, Frey et al. 2003, 2005; J2228+0110 at $z = 5.95$, Cao et al. 2014; J1427+3312 at $z = 6.12$, Frey et al. 2008; J1429+5447 at $z = 6.21$, Frey et al. 2011). Imaging observations of these mJy-level weak radio sources largely benefit from the high sensitivity offered by the large apertures in the EVN. However, the VLBA has also been successfully used for studies of extremely high redshift AGN (Momjian et al. 2008, 2018), including the brightest ($\sim$100 mJy) source J0906+6930 at $z = 5.47$

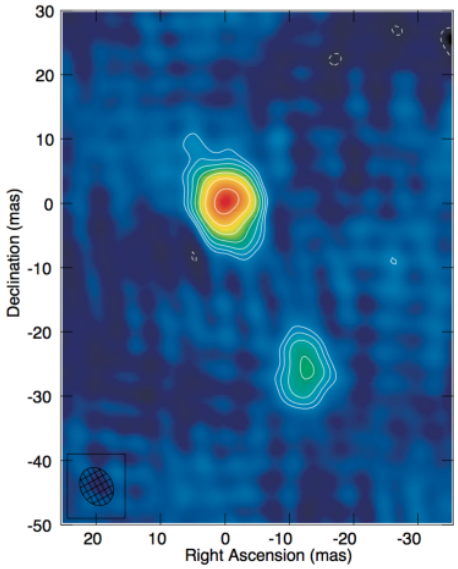

Figure 3.8: An example of a distant radio AGN with off-axis structure: the 1.6-GHz EVN image of the quasar J1427+3312 ($z = 6.12$) shows a double structure typical of young compact symmetric objects (CSOs). The positive contour levels increase by a factor of $\sqrt{2}$. The first contours are at ± 50 μJy beam^{-1}. The peak brightness is 460 μJy beam^{-1}. Credit: Frey et al. (2008), reproduced with permission ©ESO.

(Zhang et al. 2017), and even for the radio-quiet source J0100+2802 at $z = 6.33$ (Wang et al. 2017) employing long total integration time. At a somewhat lower redshift limit ($z > 4.5$), a detailed account of VLBI observations is given by Coppejans et al. (2016). At the time of writing this document, there are slightly more than 30 jetted $z > 4.5$ AGN with VLBI imaging observations available, at least at a single observing frequency. Based on sometimes sparse information on their radio spectral indices, flux density variability and brightness temperatures, the ratio of off-axis (unbeamed) jets to Doppler-boosted jets pointing close to the line of sight is about unity (Coppejans et al. 2016).

The enormous power of the most distant quasars originates from accretion onto SMBHs with billions of solar masses. The mere existence of such monsters well within 1 Gyr after the Big Bang is a serious challenge for the models that have to explain their initial formation. It is currently not understood in the framework of the ΛCDM cosmology how matter could have assembled so quickly in these black holes. Theoretical models either assume hyper-Eddington accretion rate with $> 100\,M_\odot$ seed black holes (e.g. Inayoshi et al. 2016) or a rapid creation of very massive ($\sim 10^5$ $M_\odot$) black hole seeds (e.g. Alexander & Natarajan 2014). Also unknown is the final redshift frontier of the formation of jetted AGN which could supply information on the accretion process, possibly constraining the models.

Based on growing observing evidence, its seems that blazars, i.e. radio AGN with jets nearly pointing to us, are increasingly over-abundant with respect to unbeamed jetted sources at $z > 3$ (e.g. Volonteri et al. 2011). The reason for this apparent disagreement between measurements and expectations is not found yet. Ghisellini & Sbarrato (2016) proposed a scenario where an obscuring

bubble surrounds the AGN at very high redshifts, effectively blocking the lines of sight different from those of the jet direction, preventing their optical detection and spectroscopic redshift measurements. On the other hand, a remarkable fact is that none of the five $z \approx 6$ sources imaged with VLBI to date falls into the blazar category.

Recent EVN observations of $z > 4$ blazar candidates (Cao et al. 2017) revealed two "impostors" which share the properties of blazar broad-band spectral energy distributions but their radio emission is clearly not relativistically beamed. Instead, they show nearly symmetric sub-arcsecond radio structures. This underlines the importance of VLBI measurements in providing the ultimate evidence for the blazar nature of jetted AGN.

For good statistics, we need large samples. Major advances are anticipated in the field of high-redshift AGN research in the next decades. Presently, less than 3000 objects with measured spectroscopic redshifts at $z > 4$ are known, but their number is expected to grow rapidly. For example, the Panoramic Survey Telescope & Rapid Response System 1 (Pan-STARRS1) started to deliver high-redshift discoveries (e.g. Bañados et al. 2018a). It seems that the jetted fraction of AGN does not show an obvious evolutionary trend until at least $z \approx 6$ (Bañados et al. 2015), so we can expect that nearly $\sim$10% of the new discoveries will become suitable VLBI targets. The definition of high-redshift AGN samples for radio studies critically depends on optical spectroscopic measurements and we should understand the associated selection effects.

3.2.3 Multiple supermassive black hole systems

SMBH growth through mergers: a natural consequence of galaxy evolution

Dual or binary supermassive black hole (SMBH) systems have long been predicted to be common in the Universe (Begelman et al. 1980), the expected combined result of (a) hierarchical galaxy formation (e.g. Springel et al. 2005; Schaye et al. 2015), and (b) all massive galaxies hosting a nuclear black hole (Kormendy & Richstone 1995). Their primary importance, arguably, stems from the expectation that sub-pc (more accurately, $\lesssim 0.01$ pc) binary SMBHs dominate the stochastic gravitational wave background at nHz-μHz frequencies (e.g. Wyithe & Loeb 2003; Sesana 2013). However, another major consequence of these systems is on the host galaxies themselves. Hydrodynamical simulations predict significant increases in the star formation rate and AGN accretion rate as a dual/binary SMBH pair spiral in towards one another and disrupt the neutral and ionised gas angular momentum (e.g. Mayer et al. 2007; van Wassenhove et al. 2012).

Despite this forecasted ubiquity and the predicted binary-SMBH impacts, our observations of these systems remain limited. There are still very few compelling binary/dual SMBH candidates with separations $\ll 1$ kpc (e.g. Rodriguez et al. 2006; Valtonen et al. 2008; Deane et al. 2014). The methods used to identify binary SMBH candidates are diverse, spanning the full electromagnetic spectrum, employing direct imaging, temporal variability, and spectroscopic signatures. There has been much activity in the past decade in developing new approaches; however, VLBI has always held a distinct advantage for two primary reasons, (a) its unparalleled angular resolution in astronomy, and (b) its ability to isolate regions of high brightness temperature emission while remaining insensitive to dust obscuration (e.g. An, Mohan & Frey 2018). VLBI can identify binary SMBH candidates through a number of methods, but most prominently through the imaging of two flat-spectrum radio cores, with evidence of nearby ejecta from one or both. An excellent example of this is 0402+379 (Rodriguez et al. 2006). Fainter, higher-redshift examples are expected to increase as more wide-field VLBI surveys are carried out. For example, there were two compelling binary SMBH candidates discovered in a $\sim 10\,\mu$Jy beam^{-1} survey of the COSMOS field (Herrera Ruiz et al. 2017).

Synergies with Gravitational Wave Experiments

Given the small number statistics, the properties of low separation binaries themselves are ill determined (e.g. typical binary in-spiral rates and environmental coupling at sub-kpc scales). These are important to constrain as they directly determine the low-frequency gravitational wave spectrum, particularly at nHz frequencies (Ravi et al. 2014). Indeed, without environmental coupling or host galaxy triaxiality, binaries would take of order a Hubble time to merge via gravitational radiation alone, following the ejection of most matter within binary orbital separations of $\sim$1 parsec (Merritt & Milosavljević 2005). Statistics from a large sample of binaries will measure the in-spiral rate and directly address the question of whether binaries 'stall' or not (Burke-Spolaor 2011).

In-spiral rates are also determined by orbital eccentricity. As shown in a number of studies (e.g. Sesana 2013; Ravi et al. 2014), stellar scattering driven models predict that if typical binary SMBHs have an initial eccentricity of $e_0 \sim 0.7$ at formation, the expected characteristic strain at 1 nHz is suppressed by a factor of a few. This of course has significant impact on the detectability timescale of the GW signal with current and future pulsar timing array experiments. Therefore, direct constraints from an EM perspective are critically important in attempts to find consistency between black hole growth models, merger rates, and gravitational wave signal detections (or the lack thereof).

In addition to the contribution towards and benefit from pulsar timing array results, VLBI could play an important role in understanding the lower-mass SMBH in-spiral and merger rate. The number of merger events detected by *LISA* in the $10^{-4.5} \lesssim \nu_{\rm GW} \lesssim 10^{-2}$ range will need to be reconciled with the number of spatially-resolved systems in the corresponding mass range of $M_{\rm BH} \sim 10^{5-7}\,{\rm M}_{\odot}$ (Schaye et al. 2015), for lower redshifts where these correspondingly lower luminosity systems might be detectable with VLBI. This will require sensitivity enhancements or increased observing time on VLBI arrays, given the lower mass black holes. Our window of the gravitational wave Universe is set to expand dramatically over the next 1-2 decades and VLBI stands poised to play an important role across the GW spectrum.

Leveraging off the radio survey revolution: VLBI follow-up of binary candidates from arcsec-scale imaging

Deep, wide-area surveys at arcsec-scales with new and upgraded radio telescopes are set to revolutionise our view of the radio sky. The log-spiral configurations and large numbers of antennas in new instruments such as MeerKAT and SKA1-MID result in dramatic image fidelity improvements. These traits combined with sheer number of sources expected to be detected will result in new opportunities in the search for exotic radio-jet morphologies, most ably performed using machine learning techniques (Aniyan & Thorat 2017). A subset of these outlier sources may well be caused by binary SMBH-induced precession (orbital or geodetic, e.g. Kaastra & Roos 1992; Krause et al. 2019) as well as mergers (e.g. Merritt & Ekers 2002; Krause et al. 2019). VLBI will be critical in following up this these large samples of exotic radio source morphologies.

Simulations of gas-rich systems suggest that the in-spiral from $\sim$1000 to $<$1 parsec takes of order several Myr (Blecha et al. 2011; van Wassenhove et al. 2012), which is well-matched to a typical radio jet synchrotron lifetime time of order $\sim 10-100$ Myr. Therefore, multiple modulations of the jet axis should be present in a select number of systems. An excellent example of binary-induced precession is possibly seen in Cygnus A (see Fig.3.9), the archetype radio FR-II radio galaxy recently found to host a kpc-scale binary SMBH (Perley et al. 2017). NGC 326 is another low-redshift example thereof, featuring S-shaped jets (or X-shaped, depending on angular resolution and projection effects) that are very likely caused by the presence of a kpc-scale and spatially-resolved black-hole pair (e.g. Merritt & Ekers 2002).

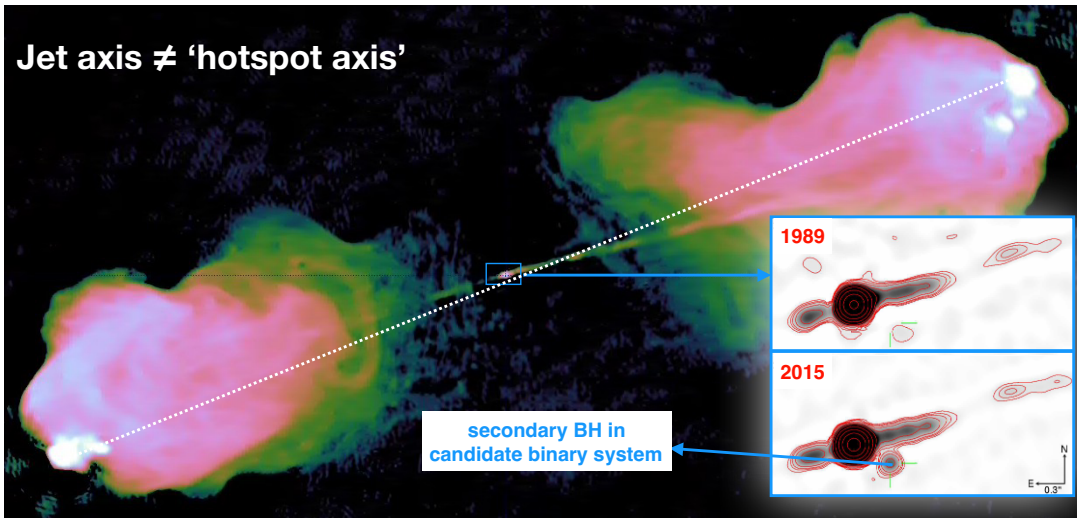

Figure 3.9: Cygnus A (image credit: Smirnov & Perley) jet axis appears misaligned with the vector between the brightest hot spots (white dashed line) – due to precession? (inset) Appearance of a transient radio source indicaties that Cygnus A is in a binary SMBH system (Perley et al. 2017). ©AAS. Reproduced with permission.

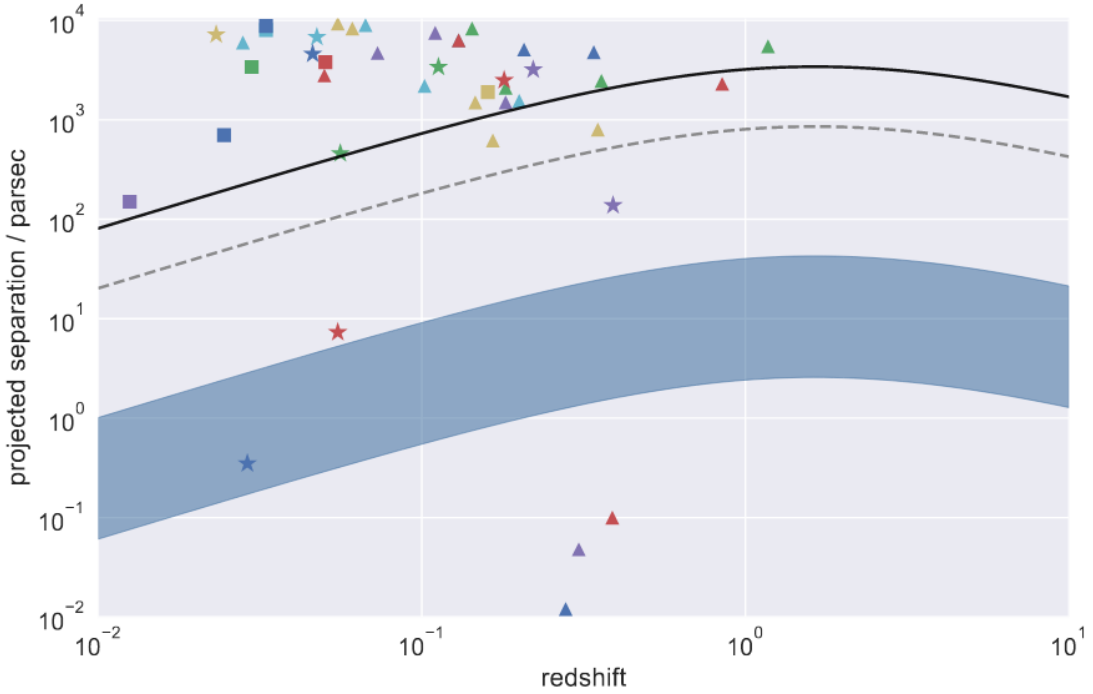

Figure 3.10: Image modified from Deane et al. (2015). Sample of dual/binary AGN candidates as revealed by X-ray (squares), optical/infrared (triangles) and radio (stars) wavelengths. Spatial resolution limits: EVN (for frequency range 1-22 GHz), dark blue region; *HST* – dashed grey line; *Chandra* – solid black line.

All the above examples suggest that a close-pair (∼kpc-scale) dual/binary SMBH could in principle be discovered using the signature modulations imprinted onto the radio jets. Recently, Krause et al. (2019) performed a systematic search for precessing jets in the 3CRR sample (Lang et al. 1983), as well as a few other well-known radio sources. They find such evidence wide-spread, which, if interpreted as a signpost for binary SMBHs, points toward this being a valid tracer thereof. The striking assertion made by Krause et al. (2019) is that the majority of powerful radio sources host binary SMBHs, based on morphological traits consistent with geodetic precession. They make the case for why jet precession should be predominantly driven by binary black-hole systems, rather than jet-cloud interaction, peculiar velocity with respect to an intracluster medium, or tri-axiality of the host halo. The set of signature traits for jet precession will be readily detected in vast numbers, making VLBI critical to test this assertion and potentially expand this window into binary SMBH formation and evolution.

The role of VLBI in multiple SMBH research

VLBI has a unique and critical role to play in directly imaging binary SMBH systems towards GW-relevant separations ($\lesssim 0.01$ pc). As is seen in Fig. 3.10, VLBI is able to probe down to $\sim$ pc-scale separation for all redshifts and into the pulsar timing array sensitivity band for low-z targets with high-frequency imaging. The projected separation lower limit in the figure is set to binary SMBH separations with gravitational wave frequencies that fall into the pulsar timing array sensitivity band (for $M_{\odot} \sim 10^8\,M_{\odot}$). The parameter space between 1-100 pc, which is almost exclusively accessed by VLBI, is critical to constrain in-spiral rates, the prevalence of 'stalled binaries', and the impact on the gravitational wave spectrum, as well as SMBH growth.

The advantage of VLBI in binary AGN discovery is the superior angular resolution and its high-brightness temperature filter. However, it is important to consider VLBI's limitations in this particular science case and how these may be alleviated with technological developments and array enhancements. In the past, its disadvantages have primarily been (a) low survey speed (b) low sensitivity, (c) dynamic range limits due to poor *uv*-coverage and imperfect calibration, and, of course, (d) the fact that not all active SMBHs are jetted, let alone have compact, high-brightness temperature components. Many of these limitations will be or to some extent have been significantly mitigated, posing a bright future for multiple SMBH searches with VLBI arrays. In order to identify these seemingly rare systems, wide-field surveys will need to become a more commonly used VLBI observing mode - both for contiguous surveys of legacy multiwavelength fields as well as targeted follow-up of promising samples (e.g. radio-jet or optical host morphology selected).

Just as for the inner-most regions of AGN, VLBI studies of multiple SMBHs require multi-band and polarimetric imaging across about a decade of frequency coverage ($\sim 1-20$ GHz), to ensure the nature of emission components can be decoupled from one another, as well as utilising the angular resolution lever arm of high frequencies to probe smaller separation binaries. This science case will also greatly benefit from wide-band feeds for in-band spectral indices. The higher fractional bandwidths will provide improved *uv*-coverage and hence imaging fidelity and dynamic range, which in turn provide better deconvolution performance. These are crucial aspects for systems with a very faint secondary component.

While VLBI has a number of spectacular examples of binary SMBH candidates, the expectation is that array, technology, and technique enhancements will lead to these outlier examples becoming common-place in the coming 1-2 decades. This will not only serve to improve our understanding of black hole and galaxy evolution models, but more closely tie electromagnetic and gravitational wave observations of the Universe together.

3.2.4 Intermediate-mass black holes

The finding of quasars powered by SMBHs of 10^9 $M_\odot$ when the Universe was only 0.7 Gyr old (e.g. Mortlock et al. 2011; Wu et al. 2015; Bañados et al. 2018b) suggests that these had to grow from seed black holes of 100-10^5 $M_\odot$ via accretion and merging (Volonteri et al. 2003). Such seed black holes could form from the death of the first generation of (Population III) stars, from direct collapse of gas in protogalaxies, or from mergers in dense stellar clusters (e.g. Volonteri 2010; Mezcua 2017). Detecting these early Universe seed black holes poses an observational challenge; however, the leftovers of those seeds that did not become supermassive should be found in the local Universe as intermediate-mass black holes (IMBHs) with $100 < M_{\rm BH} < 10^6$ $M_\odot$.

A myriad of studies have hence focused on searching for IMBHs in the local Universe. The first searches aimed at globular clusters, where several IMBH candidates have been proposed based on dynamical mass measurements and pulsar accelerations (e.g. Gebhardt et al. 1997, 2002; Lützgendorf et al. 2013; Kızıltan et al. 2017). However, no conclusive detections of accretion signatures have been achieved (e.g. Wrobel et al. 2015) even when reaching rms sensitivities of $\sim 1\mu$Jy beam^{-1} via stacking of the VLA radio images of 24 globular clusters (Tremou et al. 2018).

Dwarf galaxies with quiet merger and accretion histories are thought to be the best analogues of the first galaxies and therefore an excellent place where to look for the relics of the early Universe seed black holes. A few hundreds of IMBH candidates have been found in dwarf galaxies as low-mass AGN ($M_{\rm BH} \lesssim 10^6$ $M_\odot$) based on optical (e.g. Greene & Ho 2004, 2007; Reines et al. 2013; Baldassare et al. 2015; Chilingarian et al. 2018) and infrared (Satyapal et al. 2008; Sartori et al. 2015; Marleau et al. 2017) emission line diagnostics or the detection of X-ray emission (e.g. Schramm et al. 2013; Lemons et al. 2015; Baldassare et al. 2017; Mezcua et al. 2016, 2018a). In galaxies having recently undergone a minor merger, such IMBHs would be off-nuclear and be detected as ultraluminous X-ray sources (e.g. Farrell et al. 2009; Bellovary et al. 2010; Webb et al. 2012; Mezcua et al. 2013a,b, 2015, 2018b). Very few systematic studies have however been carried out in the radio regime (e.g. Greene et al. 2006).

Detecting jet radio emission from IMBHs/low-mass AGN can tell us about their accretion physics, jet efficiency and power, and whether they are able to impart mechanical feedback on their hosts (i.e. hampering or triggering star formation) as more massive radio galaxies do (e.g. McNamara & Nulsen 2007, 2012; Tadhunter et al. 2014; Morganti et al. 2015; Maiolino et al. 2017). The finding that AGN feedback from IMBHs significantly impact the formation of stars in their host dwarf galaxies and thus the amount of material available for the IMBH to grow would have strong implications for seed BH formation models, as it would imply that the local IMBHs/low-mass AGN so far detected might not be the relics of the early Universe seed BHs (Mezcua 2019). Very few of the IMBHs/low-mass AGN found in dwarf galaxies or ultraluminous X-ray sources do however show jet radio emission (Greene et al. 2006; Wrobel & Ho 2006; Wrobel et al. 2008; Mezcua & Lobanov 2011; Nyland et al. 2012, 2017; Reines & Deller 2012; Webb et al. 2012; Mezcua et al. 2013a,b; Reines et al. 2014; Mezcua et al. 2015, 2018a,b). The radio fluxes of these sources barely reach more than 1 mJy at the sub-arcsecond angular resolutions of the VLA, which makes detecting and resolving the radio emission on VLBI milli-arcsecond scales extremely challenging (e.g. Greene et al. 2006; Wrobel & Ho 2006; Reines et al. 2011, 2014; Mezcua & Lobanov 2011; Mezcua et al. 2013a,b, 2015; Nyland et al. 2012; Reines & Deller 2012; Paragi et al. 2014). In order to disentangle core and jet radio emission and search for outflow morphologies at VLBI scales we need μJy sensitivities, which would be achievable with the implementation of wide-band receivers in the EVN facilities. This would allow us to probe whether, similarly to SMBHs, jets are also produced

and collimated on sub-parsec scales in IMBHs, supporting the universality of the accretion physics at all mass scales, and thus to apply the fundamental plane of black hole accretion to estimate the black hole mass for those sources with core radio emission (e.g. Gültekin et al. 2009, 2019; Plotkin et al. 2012). In the case of globular clusters, the μJy sensitivities would allow us to search for IMBH accretion signatures without the need of multiple observations and posterior stacking techniques (e.g. Tremou et al. 2018).

3.2.5 Requirements and synergies – the role of the EVN

As in most fields of astrophysics, observations at multiple wavebands are necessary to paint a full picture of the processes in the early Universe. Radio AGN can also serve as illuminating background sources for HI 21-cm absorption studies of the intergalactic medium around the epoch of reionisation. The unique role of VLBI continues to be the ability of high-resolution imaging of jetted sources. Milliarcsecond-scale compact radio structure is conventionally used as the best evidence for jetted AGN activity, even at very low accretion rates. The improving sensitivity and/or the extension of the available observing time at the EVN would be desirable to allow for a survey of a sizeable sample of traditionally "radio-quiet" sources from these enormous distances. An increase of the length of EVN observing sessions would leave more room for studies of newly-discovered high-redshift sources. Optical spectroscopic discoveries e.g. with the James Webb Space Telescope (*JWST*) Near-Infrared Spectrograph (NIRSpec) will certainly cover the southern sky as well. Because of their geographic locations, most EVN stations will be in a unique position for co-observing with the upcoming SKA and its precursor MeerKAT. The VLBI capabilities with the SKA (Paragi et al. 2015, Agudo et al. 2015) would be essential not only for the sensitivity increase but also for a better *uv*-coverage at low/southern declinations.

REFERENCES

Acciari, V.A. et al., 2010, *ApJ*, **716**, 819,
Ackermann, M. et al., 2011, *ApJ*, **743**, 171
Agudo, I. et al., 2011, *ApJ*, **726**, 13
Agudo, I. et al., 2015, *PoS["AASKA14"]093*
Alexander, T., & Natarajan, P., 2014, *Science*, **345**, 1330
An, T., Mohan, P., & Frey, S., 2018, *Radio Sci.*, **53**, 1211
Aniyan, A.K., & Thorat, K., 2017, *ApJS*, **230**, 20
Arshakian, T.G. et al., 2010, *MNRAS*, **401**, 1231
Atwood, W. B. et al., 2009, *ApJ*, **697**, 1071
Baldassare et al. 2015, *ApJL*, **809**, L14
Baldassare et al. 2017, *ApJ*, **836**, 20
Bañados, E. et al., 2015, *ApJ*, **804**, 118
Bañados, E. et al., 2018a, *ApJ*, **861**, L14
Bañados, E. et al., 2018b, *Nature*, **553**, 473
Baczko, A.-K., et al., 2016, *A&A*, **593**, A47
Begelman, M.C., Blandford, R.D., & Rees, M.J., 1980, *Nature*, **287**, 307
Bellovary et al. 2010, *ApJL*, **721**, L148
Blandford, R.D., & Königl, A., 1979, *ApJ*, **232**, 34
Blandford, R.D., & Payne, 1982, *MNRAS*, **199**, 883

Blandford, R.D., & Znajek, R.L., 1977, *MNRAS*, **179**, 433
Blecha, L. et al., 2011, *MNRAS*, **412**, 2154
Boccardi, B. et al., 2017, *A&ARv*, **25**, 4
Burke-Spolaor, S., 2011, *MNRAS*, **410**, 2113
Camenzind, M., 2005, *Mem. SAIt*, **76**, 98
Cao, H.-M. et al., 2014, *A&A*, **563**, A111
Cao, H.-M. et al., 2017, *MNRAS*, **467**, 950
Chael, A., Narayan, R., & Johnson, M.D., 2019, *MNRAS*, **486**, 2873
Chilingarian et al. 2018, *ApJ*, **863**, 1
Chirenti, C., & Rezzolla, L., 2016, *Phys. Rev. D*, **94**, 084016
Coppejans, R. et al., 2016, *MNRAS*, **463**, 3260
Deane, R.P. et al., 2014, *Nature*, **511**, 57
Deane, R.P. et al., 2015, *PoS[AASKA14]151*
Dodson, R. et al., 2017, *NewAR*, **79**, 85
Doeleman S.S., et al., 2012, *Science*, **338**, 355
Farrell et al. 2009, *Nature*, **460**, 73
Fendt, C., 2011, *ApJ*, **737**, 43
Frey, S. et al., 2003, *MNRAS*, **343**, L20
Frey, S. et al., 2005, *A&A*, **436**, L13
Frey, S. et al., 2008, *A&A*, **484**, L39
Frey, S. et al., 2011, *A&A*, **531**, L5
Frey, S. et al., 2015, *MNRAS*, **446**, 2921
Fromm, C. et al., 2013, *A&A*, **557**, A105
Gabuzda, D., Reichstein, A.R., & O'Neil, E.L., 2014, *MNRAS*, **444**, 172
Gebhardt et al. 1997, *AJ*, **113**, 1026
Gebhardt et al. 2002; *ApJL*, **578**, L41
Ghisellini, G., & Tavecchio, F., 2009, *MNRAS*, **397**, 985
Ghisellini, G. et al., 2013, *MNRAS*, **432**, 2818
Ghisellini, G. et al., 2015, *MNRAS*, **452**, 3457
Ghisellini, G. et al., 2014, *MNRAS*, **440**, 111
Ghisellini, G., & Sbarrato, T., 2016, *MNRAS*, **461**, L21
Giovannini, G. et al., 2018, *Nat. Astron.*, **2**, 472
Gómez, J.L. et al., 2016, *ApJ*, **817**, 96
Greene, J. A., & Ho, L. C., 2004, *ApJ*, **610**, 722
Greene, J. A., Ho, L. C., & Ulvestad, J. S., 2006, *ApJ*, **636**, 56
Greene, J. A., & Ho, L. C., 2007, *ApJ*, **670**, 92
Gültekin et al. 2009, *ApJ*, **706**, 404
Gültekin et al. 2019, *ApJ*, **871**, 80
Hada, K. et al., 2014, *ApJ*, **788**, 165
Han, S.-T. et al., 2013, *PASP*, **125**, 539
Hardee, P.E., Mizuno, Y., & Nishikawa, K.-I., 2007, *Ap&SS*, **311**, 281
Herrera Ruiz, N. et al., 2017, *A&A*, **607**, A132
Inayoshi, K., Haiman, Z., & Ostriker, J.P., 2016, *MNRAS*, **459**, 3738
Jorstad S., et al., 2013, *ApJ*, **773**, 147
Jung, T.H., et al., 2015, *Journal of Korean Astron. Society*, **48**, 277
Kaastra, J.S., & Roos, N., 1992, *A&A*, **254**, 96

Kim, J.-Y. et al., 2018, *A&A*, **616**, A188
Kızıltan et al. 2017, *Nature*, **542**, 203
Komissarov, S.S. et al. 2007, *MNRAS*, **380**, 51
Kormendy, J., & Richstone, D., 1995, *ARA&A*, **33**, 581
Kovalev, Y.Y. et al., 2008, *A&A*, **483**, 759
Krause, M.G.H. et al., 2019, *MNRAS*, **482**, 240
Laing, R.A., Riley, J.M., & Longair, M.S., 1983, *MNRAS*, **204**, 151
Lemons et al. 2015, *ApJ*, **805**, 12
León-Tavares, J. et al. 2010, *ApJ*, **715**, 355
León-Tavares, J. et al. 2013, *ApJ*, **763**, 36
Lobanov, A.P., 1998, *A&A*, **370**, 90
Lobanov, A.P., 2017, *Nat. Astron.*, **1**, 69
Lu, R.-S., et al., 2018, *ApJ*, **859**, 60
Lützgendorf et al. 2013, *A&A*, **552**, A49
Lyubarsky, Y., 2009, *ApJ*, **698**, 1570
Maiolino et al. 2017, *Nature*, **544**, 202
Marleau et al. 2017, *A&A*, **602**, A28
Marscher, A.P., 2014, *ApJ*, **780**, 87
Martí-Vidal, I. et al., 2015, *Science*, **348**, 311
Mayer, L., 2007, *Science*, **316**, 1874
McNamara, B. R., & Nulsen, P. E. J., 2007, *ARA&A*, **45**, 117
McNamara, B. R., & Nulsen, P. E. J., 2012, *NJPh*, **14**, 055023
Meier, D.L., 2009, *ASP Conf. Ser.*, **402**, 342
Melia, F., Yennapureddy, M.K. 2018, *MNRAS*, **480**, 2144
Merloni, A., Fabian, A.C., 2002, *MNRAS*, **332**, 165
McKinney, J.C., 2006, *MNRAS*, **368**, 1561
Merritt, D., & Ekers, R.D., 2002, *Science*, **297**, 1310
Merritt, D., & Milosavljević, M., 2005, *Living Reviews in Relativity*, **8**, 8
Mertens, F. et al., 2016, *A&A*, **595**, A54
Mezcua, M., 2017, *IJMPD*, **26**, 1730021
Mezcua, M., 2019, *Nat. Astr.*, **3**, 6
Mezcua, M., & Lobanov, A. P., 2011, *AN*, **332**, 379
Mezcua, M. et al. 2013a, *MNRAS*, **436**, 1546
Mezcua, M. et al. 2013b, *MNRAS*, **436**, 3128
Mezcua, M. et al. 2015, *MNRAS*, **448**, 1893
Mezcua, M. et al. 2016, *ApJ*, **817**, 20
Mezcua, M. et al. 2018a, *MNRAS*, **478**, 2576
Mezcua, M. et al. 2018b, *MNRAS Letters*, **480**, L74
Molina, S.N. et al., 2014, *A&A*, **566**, A26
Momjian, E., Carilli, C.L., & McGreer, I.D., 2008, *AJ*, **136**, 344
Momjian, E. et al., 2018, *ApJ*, **861**, 86
Morganti, R. et al. 2015, *A&A*, **580**, A1
Mortlock, D. et al. 2011, *Nature*, **474**, 616
Mościbrodzka, M. et al. 2016, *A&A*, **586**, A38
Nakamura, M. et al., 2018, *ApJ*, **868**, 146
Nyland, K. et al. 2012, *ApJ*, **753**, 103

Nyland, K. et al. 2017, *ApJ*, **845**, 50
Padovani, P., 2017, *Nature Astron.*, **1**, 194
Paragi, Z. et al. 2014, *ApJ*, **791**, 2
Paragi, Z. et al., 2015, *PoS["AASKA14"]143*
Perley, D.A. et al., 2017, *ApJ*, **841**, 117
Plavin, A.V., et al., 2019, *MNRAS*, **485**, 1822
Plotkin, R. M. et al. 2012, *MNRAS*, **419**, 267
Pushkarev, A.B. et al., 2012, *A&A*, **545**, A113
Ravi, V. et al., 2014, *MNRAS*, **442**, 56
Reines, A. E., & Deller, A. T., 2012, *ApJL*, **750**, L24
Reines, A. L. et al. 2011, *Nature*, **470**, 66
Reines, A. L. et al. 2013, *ApJ*, **775**, 116
Reines, A. L. et al. 2014, *ApJL*, **787**, L30
Rioja, M. et al., 2015, *AJ*, **150**, 202
Rodriguez, C., 2006, *ApJ*, **646**, 49
Satyapal, S. et al. 2008, *ApJ*, **677**, 926
Sartori, L. F. et al. 2015, *MNRAS*, **454**, 3722
Sbarrato, T. et al., 2012, *MNRAS*, **426**, 91
Sbarrato, T. et al., 2013, *ApJ*, **777**, 147
Sbarrato, T. et al., 2015, *MNRAS*, **446**, 1483
Schaye, J. et al., 2015, *MNRAS*, **446**, 521
Schinzel, F. et al., 2012, *A&A*, **537**, A70
Schramm, M. et al. 2013, *ApJ*, **773**, 150
Sesana, A., 2013, *MNRAS*, **433**, L1
Shen, Y. et al., 2011, *ApJS*, **194**, 45
Springel, V., 2005, *Nature*, **435**, 629
Tadhunter, C. N. et al. 2014, *Nature*, **511**, 440
Tremou, E. et al. 2018, *ApJ*, **862**, 16
Tuccari, G. et al., 2017, *Proc. 23 EVGA Meeting*, (Gothenburg), 81
Valtonen, M.J., 2008, *Nature*, **452**, 851
van Wassenhove, S. et al., 2012, *ApJ*, **748**, L7
Volonteri, M., 2010, *A&ARv*, **18**, 279
Volonteri, M. et al. 2003, *ApJ*, **582**, 559
Volonteri, M. et al., 2011, *MNRAS*, **416**, 216
Walker, R.C. et al. 2018, *ApJ*, **855**, 128
Wang, R. et al. 2017, *ApJL*, **835**, L20
Webb, N. A. et al. 2012, *Science*, **337**, 554
Wilott ,C.J. et al., 2010, *AJ*, **139**, 906
Wrobel, J. M., & Ho, L. C. 2006, *ApJL*, **646**, L95
Wrobel, J. M. et al. 2008, *ApJ*, **686**, 838
Wrobel, J. M. et al. 2015, *AJ*, **150**, 120
Wu,X.-B. et al. 2015, *Nature*, **518**, 512
Wyithe, J.S.B., & Loeb, A., 2003, *ApJ*, **590**, 691
York, D.G. et al., 2000, *AJ*, **120**, 1579
Zamaninasab, M. et al., 2014, *Nature*, **512**, 126
Zhang, Y. et al., 2017, *MNRAS*, **468**, 69